A 5′ cytosine binding pocket in Puf3p specifies regulation of mitochondrial mRNAs

Deyu Zhu[a,1], Craig R. Stumpf[b,1], Joseph M. Krahn[a], Marvin Wickens[b,2], and Traci M. Tanaka Hall[a,2]

[a]Laboratory of Structural Biology, National Institute of Environmental Health Sciences, Research Triangle Park, NC 27709; and [b]Department of Biochemistry, University of Wisconsin-Madison, Madison, WI 53706

A single regulatory protein can control the fate of many mRNAs with related functions. The Puf3 protein of *Saccharomyces cerevisiae* is exemplary, as it binds and regulates more than 100 mRNAs that encode proteins with mitochondrial function. Here we elucidate the structural basis of that specificity. To do so, we explore the crystal structures of Puf3p complexes with 2 cognate RNAs. The key determinant of Puf3p specificity is an unusual interaction between a distinctive pocket of the protein with an RNA base outside the "core" PUF-binding site. That interaction dramatically affects binding affinity in vitro and is required for regulation in vivo. The Puf3p structures, combined with those of Puf4p in the same organism, illuminate the structural basis of natural PUF-RNA networks. Yeast Puf3p binds its own RNAs because they possess a −2C and is excluded from those of Puf4p which contain an additional nucleotide in the core-binding site.

crystal structure | RNA | translational regulation

Control of mRNA stability, translation, and location are pervasive. Elements in the 3′-UTR interact with regulatory proteins to confer regulation. New networks of control have begun to emerge from analyses of regulatory proteins, their targets, and their biological functions; for example, webs of interacting 3′-UTR regulatory proteins and mRNAs control stem cells in *Caenorhabditis elegans* (1, 2), the cell cycle during oocyte maturation and early development in *Xenopus* (2–4), and RNA regulation in neurons (5).

The yeast Puf3 protein and mitochondrial mRNAs provide a particularly dramatic example of a single protein that binds and regulates a large number of functionally related mRNAs. In the budding yeast, *Saccharomyces cerevisiae*, many nuclear-encoded mRNAs with mitochondrial functions contain a conserved sequence in their 3′-UTRs (6) that binds Puf3p (7). Indeed, many mRNAs of mitochondrial function coimmunopurify with Puf3p from yeast extracts (8). Loss of this single PUF protein impairs mitochondrial morphology and maintenance (9) and disrupts localization of its target mRNAs to the vicinity of mitochondria (10). Puf3p binds to and destabilizes *COX17* mRNA, which encodes a copper metallochaperone involved in the biogenesis of the mitochondrial respiratory complex (7, 11, 12). Thus, by controlling a large battery of mRNAs, this single PUF protein is vital for regulation of the organelle.

Puf3p is a member of the PUF family of 3′-UTR–binding proteins, which regulate translation and mRNA degradation in diverse eukaryotes (13, 14). Typically, PUF proteins use 8 structural repeats to bind to RNA sequences containing a UGUR sequence (R, purine) at the 5′ end and more variable 3′ sequences (8, 13, 15–24). Each of 8 α-helical repeats contacts primarily a single base (21, 25, 26). Although Puf3p is very similar to other PUF proteins and has most of the same residues that contact RNA in other PUF proteins, it selectively interacts with and controls mitochondrial mRNAs.

We sought to understand the structural basis of the specificity of Puf3p for mitochondrial mRNAs. To do so, we analyzed the structure of Puf3p bound to 2 sites in one of its mRNA targets, *COX17*, analyzed this interaction biochemically, and tested the biological importance of the RNA base at the −2 position for regulation in vivo.

Results

General Puf3p Architecture and the Core Region. Crystal structures of the RNA-binding domain of Puf3p in complex with the *COX17* mRNA sequences for binding site A, CU**UGUA**UAUA, and site B, CC**UGUA**AAUA (Fig. 1*A*), were determined at a resolution of 3.2 and 2.5 Å, respectively. Puf3p interacts with the 8 bases of *COX17* mRNA starting from the conserved UGUA sequence much as human Pumilio1 (PUM1) binds to the equivalent RNA [Fig. 1*B* and supporting information (SI) Fig. S1] (21). The Puf3p and PUM1 structures are very similar [root mean squared deviation (RMSD) of 1.3 Å over 307 CA atoms] with equivalent curvatures; neither is flattened or twisted like Puf4p and FBF (refs. 26 and 43; Fig. S2).

The structures of Puf3p in complex with *COX17* site A and site B RNA sequences are nearly identical, with an RMSD of 0.2 Å over 343 CA atoms. The backbone structure of the RNA is different for the 2 sequences at positions 5 and 6 (Fig. 1*B*), however. [As a convention, here we number the PUF protein RNA recognition sequences beginning with the 5′ uracil (U1) of the conserved UGU sequence.] The ribose group at position 5 in the site B RNA is in a C2′-endo conformation, and A5 and A6 are presented in a *syn* orientation rather than in the typical *anti* orientation (Fig. 2*A*). Thus for A5 and A6, Puf3p recognizes the Hoogsteen edge of the base instead of the Watson–Crick edge, as has been observed in previous PUF protein structures (21, 26). These structural rearrangements allow the edges of the bases of A5 and A6 in site B to align well with bases U5 and A6 in site A (Fig. S3). A hydrogen bond between Y695 and the phosphate group between A5 and A6 may facilitate this structural change. A similar sequence (UGUAAAUA) is present in the human Pumilio2 (PUM2) binding site in p38α (27). We predict that a similar RNA backbone rearrangement may be necessary for interaction with this and another p38 mRNA recognition sequence, UGUAGAUA; indeed, a tyrosine equivalent to Puf3p Y695 is conserved in PUM2.

To evaluate the functional significance of the different RNA-binding sites, we determined the binding affinity of Puf3p for *COX17* site A and site B RNAs using electrophoretic mobility shift assays (Table 1). Based on RNA saturation, 94% of the Puf3p molecules were active in RNA binding (see *Methods*).

Fig. 1. Crystal structures of the Puf3p RNA-binding domain in complex with *COX17* mRNA sequences. (*A*) Ribbon diagram of the RNA-binding domain of *S. cerevisiae* Puf3p in complex with a *COX17* site B RNA fragment (CCU-GUAAAUA). Protein repeats are colored alternately blue and gold. The RNA is colored according to atom type (carbon, white; nitrogen, blue; oxygen, red; sulfur, yellow; phosphorus, orange). Protein side chains that contact the RNA are shown. Two loop regions that were disordered in the crystal structures are indicated by dotted lines. This figure and Fig. 2 were prepared with PyMol (31). (*B*) Superposition of CA traces of the Puf3p:*COX17* site B RNA complex (blue) and PUM1:RNA complex (gray; PDB ID: 1M8Y) aligned over the entire protein structures. The *COX17* site A RNA from the structure of a complex with Puf3p is shown in gold.

Puf3p binds tightly to both RNAs, but binds ≈10-fold more tightly to site B (K_d of 3.0 nM vs. 0.31 nM). Two bases (positions −1 and 5) differ between sites A and B; thus, we tested binding to an RNA with position 5 of site B changed to a uracil (A5U site B). Comparing binding to this RNA (1.6 nM) with binding to site B, we found a 5-fold decrease in affinity when uracil is at position 5. Cytosine at position −1 results in a modest 2-fold tighter binding versus uracil at that position. The tight binding for each site is consistent with in vivo experiments demonstrating delayed

deadenylation and decay of the *COX17* transcript when either of the binding sites was destroyed (12).*

A Distinctive Binding Pocket in Puf3p. The key, and most distinctive, feature of Puf3p binding is its interaction with the conserved cytosine at the −2 position of Puf3p targets, 2 bases 5′ of the conserved UGU sequence (8) (Fig. 2*B*). This cytosine is bound by the protein in a pocket between the N-terminal ends of the RNA-binding helix of repeat 8 and the terminal helix in repeat 8′. Hydrogen bonds that appear to be specific for a cytosine are formed between the Watson–Crick edge of the base and main chain and side chain atoms of S866 and K819 (Fig. 2*B*). L864 forms a stacking interaction with the base, and the main chain nitrogen atom of A865 interacts with the 2′ OH of C(−2).

Inspecting sequence alignments, the cytosine-binding pocket is conserved in certain PUF protein homologues in budding yeast and *Aspergillus* species. Analogous pockets may be present in other proteins, but not be evident in primary sequence alignments. However, structural alignments with PUM1 and Puf4p indicate that the terminal helix and the RNA-binding helix of repeat 8 in PUM1 and Puf4p are positioned closer to each other than the equivalent helices in Puf3p, and S866 is replaced by a tyrosine in PUM1 and a histidine in Puf4p. The closer helices and bulky side chains appear to fill what would have been the additional binding pocket, precluding an analogous interaction.

To explore the importance of this additional binding pocket for RNA recognition, we first determined the binding affinity of RNAs with different bases at the −2 position (Table 1). RNAs with a uracil, guanine, or adenine at the −2 position bound ≈70-fold more weakly than the equivalent RNA with a cytosine at that position. An 8-base RNA starting from U1 (Δ5′ site B) bound ≈400-fold more weakly than the corresponding 10-base RNA. These data demonstrate that the binding pocket for the −2 position is important for high-affinity binding.

To confirm the importance of the binding pocket on the protein side, we mutated S866 to alanine and determined the binding affinity of the mutant protein for *COX17* RNA (Table 1). The mutant protein appears to be properly folded because it elutes from a gel filtration column at the same position as wild-type protein, and the circular dichroism spectra are essentially identical ([Fig. S4](#)). The S866A mutant protein bound ≈400-fold more weakly than native protein to the *COX17* site B RNA (K_d 129 nM vs. 0.31 nM), indicating that this single amino acid residue contributes critically to high-affinity binding.

Regulation by Puf3p in Vivo Requires Binding Sites with −2C. To assess whether the cytosine at the −2 position is important for regulation in vivo, we analyzed the decay of reporter mRNAs containing either wild-type or mutant forms of the *COX17* 3′-UTR. We compared the stabilities of *COX17* mRNA bearing either the wild-type 3′-UTR or a mutant 3′-UTR in which the base at −2 was changed from cytidine to adenine in both site A and site B (Table 1). (Mutation of either site disrupts binding in vitro.) Both genes were placed under control of the *GAL* promoter. To measure mRNA half-life, the genes were induced in galactose-containing media, and then repressed by the addition of glucose. Decay of the mRNA after transcriptional inhibition was quantified using Northern blot analysis (Fig. 3).

In wild-type cells, the wild-type reporter mRNA decayed rapidly (half-life of ≈4 min), similar to what was reported previously (Fig. 3*A*) (7, 12, 28, 29). The C(−2)A double mutant was stabilized approximately 4-fold in the same cells (half-life ≈17 min). In the Δ*puf3* strain, wild- type and mutant reporters were both stabilized equivalently (Fig. 3*B*; half-life ≈12 min).

Fig. 2. Recognition of RNA by the Puf3p RNA-binding domain. The protein and RNA are colored as in Fig. 1 *A*. (*A*) Puf3p recognition of bases A4–A6 in *COX17* site B RNA. (*B*) Recognition of a cytosine 2 positions 5′ of the conserved UGUA sequence.

BIOCHEMISTRY

Table 1. RNA-binding analyses of wild-type and mutant Puf3p

Protein	RNA	RNA sequence 12345678*	K_d (nM)	K_{rel}[†]
Puf3p	*COX17* site A	CUUGUAUAUA	3.0 ± 0.3	1
Puf3p	*COX17* site B	C**C**UGUA**A**AUA	0.31 ± 0.07	0.1[‡]
Puf3p	A5U site B	C**C**UGUAUAUA	1.6 ± 0.09	0.5[‡] (5[‡] vs. site B)
Puf3p	C(−2)U site A	**U**UUGUAUAUA	205 ± 14	68[‡]
Puf3p	C(−2)G site A	**G**UUGUAUAUA	224 ± 11	75[‡]
Puf3p	C(−2)A site A	**A**UUGUAUAUA	234 ± 9	78[‡]
Puf3p	C(−2)A site B	**A**CUGUA**A**AUA	58.3 ± 7	188[‡] (vs. site B)
Puf3p	Δ5′ site B	UGUA**A**AUA	119 ± 6	384[‡] (vs. site B)
mutPuf3p S866A	*COX17* site B	C**C**UGUA**A**AUA	129 ± 19	416[‡] (vs. site B)
Puf3p	*HO* RNA Puf4p BS	**U**GUGUAUAU**U**A	181 ± 12	60[‡]
Puf3p	*HO* RNA Mpt5p BS	**G**UUGUAU**G**UAAU	607 ± 44	202[‡]

*Numbers indicate positions in the core recognition sequence. Bases that differ from the sequence of *COX17* site A RNA are in bold.

[†]K_{rel} reports the affinity of wild-type or mutant Puf3p for the RNA sequence, relative to the affinity of wild-type Puf3p for *COX17* site A RNA, unless indicated otherwise in parentheses.

[‡]Asterisks denote statistically significant differences ($P < .05$).

These data permit 2 conclusions: (*i*) The presence of a C at the −2 position is important for biological regulation in vivo (Fig. 3*A*),and (*ii*) the effect of the −2 base is dependent on Puf3p (Fig. 3*B*).

Bioinformatic analysis supports the biological importance of the cytosine at −2. Cytosine was enriched at the −2 position among the mRNAs associated with Puf3p in coimmunopurification experiments; 82% of the mRNAs (144 of 174) associated with Puf3p had a −2C, compared with the 18% prevalence of cytosine in the yeast genome ($P = 1.37 \times 10^{-77}$). Indeed, the cytosine at −2 was part of the binding motif initially identified simply as a conserved sequence in the 3′-UTRs of mitochondrial mRNAs (6) and later shown to bind Puf3p (7, 8). The cytosine at −2 is evolutionarily conserved as well. To examine conservation, we analyzed homologs of the mRNAs that bind Puf3p in *S. cerevisiae* (8) in related yeast species (*S. paradoxus, mikatae, bayanus, castellii, kudriavzevii,* and *kluyveri*). A cytosine at −2 is more highly conserved among these species than are the rare A, G, or U identities ($P = .001$). A cytosine at −2 also is enriched in mRNAs that demonstrate a strict dependence on Puf3p for localization to mitochondria ($P = .0001$) (9). In summary, both the effects on RNA stability and the conservation of the −2C support the view that the −2C is important for Puf3p function in vivo.

Puf3p Versus Puf4p: Two Determinants of Binding and Exclusion. The Puf3p-RNA structures suggest how different PUF proteins expressed in the same cell can specifically regulate only their own RNA target sequences. Puf3p binds ≈60-fold more weakly to the Puf4p-binding site in *HO* RNA and ≈200-fold more weakly to the Mpt5p-binding site in *HO* RNA compared with *COX17* site A (Table 1). Both Puf4p and Mpt5p target sequences lack a −2C and contain inserted or mismatched bases downstream of the UGU sequence (Table 1). The crystal structure of Puf4p with RNA identified an additional base between bases 6 and 7 (referred to here as base 6′) as a key determinant for Puf4p recognition (26). Our new understanding that the key determinant for Puf3p binding is a −2C allowed us to evaluate the importance of these 2 features for selective PUF protein target recognition by Puf3p and Puf4p.

To do so, we analyzed Puf3p and Puf4p binding to a series of RNAs that transition from optimal Puf3p to optimal Puf4p-binding sites (Fig. 4; Table S1). We focused on 2 determinants: the identity of the −2 base and the presence or absence of the 6′ nucleotide (8, 26). Thus, we prepared 4 RNAs with either U or C at the −2 position and either with or without an "extra" base at 6′.

Puf3p bound tightly (K_d 3.0 nM) to an RNA that matched its optimal site, with a −2C and without a 6′ nucleotide. The presence of a cytosine at −2 enhanced binding ≈70-fold relative to an identical RNA with uracil (Fig. 4, *Top*; Table S1). Similarly, Puf3p had a ≈30-fold preference for an RNA lacking the 6′ nucleotide relative to one containing it. Puf3p bound the worst to an RNA that was suboptimal in both determinants; the presence of a −2U and a 6′ nucleotide reduced binding by ≈90-fold.

Puf4p exhibited a reciprocal pattern. It bound tightly to its optimal site (K_d 7.2 nM) but poorly to sites lacking the 6′ nucleotide (Fig. 4, *Bottom*; Table S1). Puf4p did not discriminate the identity of the −2 base: instead, it bound equivalently to −2U and −2C regardless of whether the 6′ nucleotide was present. Together, these data demonstrate that the presence of a C at −2 and the presence or absence of a 6′ nucleotide account substantially for the binding and exclusion of Puf3p and Puf4p to cognate and noncognate sites.
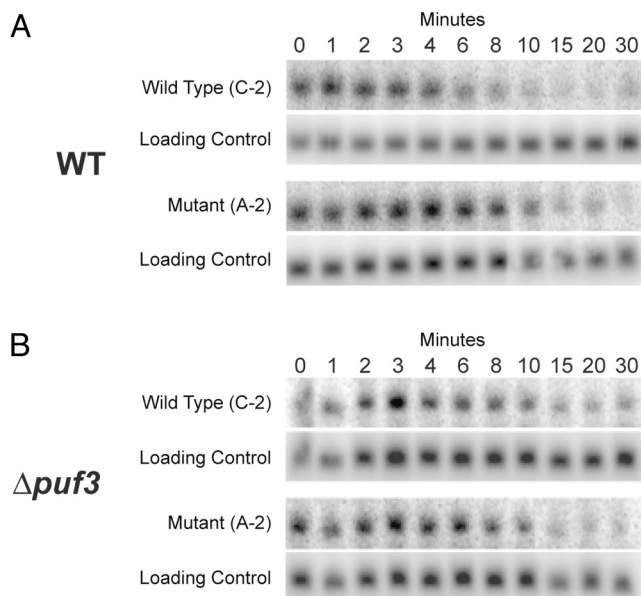

Fig. 3. A cytosine at the −2 position is critical for Puf3p-mediated mRNA decay in vivo. Representative Northern blots illustrating the decay from the steady state of *COX17* mRNAs bearing either the wild-type or mutant 3′-UTR in wild-type (*A*) and Δ*puf3* (*B*) strains. The mutant 3′-UTR carries C(−2)A mutations in both of its Puf3p-binding sites. The control RNA is ScR1.
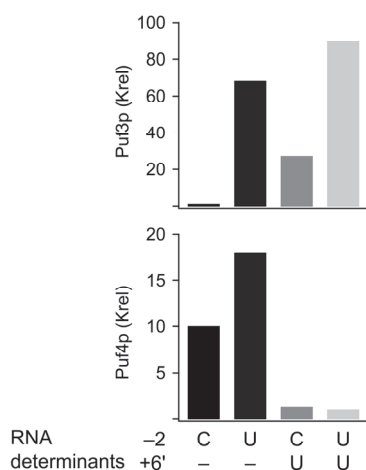
Fig. 4. Key determinants of Puf3p and Puf4p binding and exclusion. Bar graph illustrating relative binding of Puf3p and Puf4p to RNAs with either C or U at position −2 and with or without the +6′ nucleotide. RNA sequences are given in Table S1.

Discussion

Our results begin to provide a structural explanation for networks of PUF protein control in vivo. Each PUF protein must bind its own set of target RNAs and be excluded from those of other PUF proteins. A comparison of Puf3p and Puf4p is particularly instructive, because the structures of both PUF-RNA complexes are now known. These 2 PUF proteins bind almost completely nonoverlapping sets of mRNAs. Of the 213 RNAs associated with Puf3p and the 176 RNAs associated with Puf4p, only 4 associate with both proteins, and those 4 mRNAs have 2 separate elements for each protein (8). The data reported here permit a structural model of binding and exclusion of these 2 PUF proteins. Puf3p requires a cytosine in the −2 position for high-affinity binding, and that cytosine is accommodated by a specific binding pocket in repeats 8 and 8′ of the protein (Fig. 5). In Puf4p, the would-be pocket is disrupted by a histidine residue and a change in orientation of 2 α-helices; indeed, Puf4p shows no preference for a C at −2 (Figs. 4 and 5; Table S1). Consistent

with this, the −2 position is a cytosine in 82% of RNAs (144 of 174) immunopurified with Puf3p that have an identifiable binding site, but in only 12% (16 of 135) of those that bind Puf4p (8). Conversely, Puf4p targets have an additional nucleotide between positions 6 and 7. The presence of this nucleotide enhances the binding of Puf4p and diminishes binding of Puf3p (Figs. 4 and 5; Table S1). This permits Puf4p to bind to its targets, while excluding Puf3p. We suggest that Puf3p's specificity ensures that a battery of mitochondrial mRNAs are coordinately controlled, and that other mRNAs are excluded from that regulation.

Some mRNAs (18%) that are associated with Puf3p in extracts have a nucleotide other than C at the −2 position (8). The stabilities of 2 such mRNAs, *COX15* and *PET117*, have been examined and found to be unaffected by the deletion of *puf3* (8, 30). Nonetheless, mRNAs of this type may still use Puf3p for processes other than decay, such as translational repression or localization.

The studies reported here and in the accompanying paper illustrate the versatility of PUF protein specificity and affinity. In the cases of FBF and yeast Puf4p, the protein imposes a requirement for an extra base relative to PUM1, and that base flips out away from the protein. In Puf3p, a specific binding pocket imposes a requirement for a cytosine at the −2 position. Indeed, biological regulation by Puf3p requires the high-affinity interaction due to the additional binding pocket. These permutations of PUF scaffolds enable PUF proteins to bind mutually exclusive sets of RNAs yet use largely overlapping sets of atomic contacts to do so.

Methods

Protein Expression and Purification. A cDNA encoding the RNA-binding domain of Puf3p (amino acid 511–879) was amplified by PCR from *S. cerevisiae* genomic DNA and inserted into the pTYB3 expression plasmid (New England Biolabs) using NcoI and SapI restriction sites. The protein, in which Puf3p was fused to the N terminus of an intein and a chitin-binding domain, was expressed in *Escherichia coli* strain BL21(DE3) with 1 mM IPTG for 6 h at 33 °C. Bacterial pellets were resuspended in sonication buffer (20 mM sodium phosphate [pH 8.0], 500 mM NaCl) and lysed by sonication in an ice bath after the addition of 1 complete EDTA-free protease inhibitor tablet (Roche). The fusion protein was purified from the soluble fraction by incubation with chitin agarose resin (New England Biolabs) for 40 min at 4 °C. The resin was washed extensively with sonication buffer, then with high-salt buffer (20 mM sodium phosphate [pH 8.0], 1 M NaCl), and finally with a sonication buffer containing 150 mM NaCl. The resin was then transferred to a 50-mL conical tube and equilibrated with sonication buffer containing 150 mM NaCl and 100 mM DTT to initiate cleavage by the intein domain. The tube was sealed, and the resin was incubated for 2–3 days at room temperature. The beads were transferred into a 10-mL disposable column, and the cleaved Puf3p protein was collected. The beads were washed 2–3 times with a 1/4-column volume of sonication buffer with 150 mM NaCl and 50 mM DTT to collect additional cleaved protein. The eluted Puf3p protein was concentrated to ≈0.5 mg/mL, then dialyzed with column buffer [10 mM Tris-HCl (pH 7.4), 50 mM NaCl, 6 mM β-mercaptoethanol]. For Puf3p alone, the protein was loaded onto a Superdex 200 HR 10/30 column (GE Healthcare) and run at 0.5 mL/min in column buffer. Fractions containing Puf3p were pooled and concentrated to 3.5 mg/mL. For the complexes of Puf3p with RNA oligonucleotides, each RNA oligonucleotide (CCUGUAAAUA or CUUGUAUAUA; Dharmacon Research) was added at a 1:1 stoichiometry and incubated at 4 °C for 6 h before being loaded onto the Superdex 200 HR 10/30 column. Fractions containing Puf3p with RNA oligonucleotides were pooled and concentrated to a final protein concentration of ≈2 mg/mL for crystallization.

S866A mutPuf3p cDNA was made using the QuikChange site-directed mutagenesis kit (Stratagene) following the manufacturer's protocol. Mutants were confirmed by sequencing the full cDNA insert. Mutant protein was prepared as described above for the wild-type protein.

Crystallization and Data Collection. Crystallization experiments were conducted using the hanging-drop vapor-diffusion method at 4 °C, with 2-μL drops composed of 1 μL of Puf3p:RNA complex solution and 1 μL of well solution and equilibrated against 0.5 mL of well solution. For the Puf3p:*COX17* site B (CCUGUAAAUA) complex, the well solution was 22% PEG4000, 0.1 M sodium citrate (pH 5.2), and 1% dextran sulfate. Diffraction-quality crystals

Fig. 5. Structural basis of the RNA selectivity of Puf3p and Puf4p. A core PUF-RNA complex, with 8 helices (tan circles, R1–R8) aligned with 8 bases (purple hexagons, +1 to +8), depicted in the center, represents the "base" PUF-RNA structure, as seen in human PUM1 (21). The 2 key determinants for Puf3p and Puf4p are expanded above and to the right, respectively. See the text for details.

Table 2. Data collection and refinement statistics

	Puf3p:*COX17* SiteB	Puf3p:*COX17* SiteA
Data collection		
Space group	C2	C2
Cell dimensions		
a, b, c, Å	151.13, 87.07, 125.18	150.18, 87.13, 124.91
α, β, γ, degrees	90.0, 116.5, 90.0	90.0, 116.2, 90.0
Resolution, Å	50–2.50 (2.59–2.50)*	50–3.20 (3.31–3.20)
R_{sym}	0.104 (0.351)	0.153 (0.453)
I/σI	12.4 (3.5)	8.6 (2.8)
Completeness (%)	94.2 (83.4)	99.8 (99.9)
Redundancy	3.2 (2.9)	3.5 (3.4)
Refinement		
Resolution, Å	36.61–2.50	28.91–3.20
Reflections	48,055 (4,213)	23,487 (2,355)
R_{work}/R_{free}	0.2277/0.2628	0.2470/0.2966
Number of atoms	9,635	9,036
Protein	8,541	8,313
Ligand/ion	663	630
Water	431	93
B-factors	62.6	63.0
Protein	62.1	61.9
Ligand/ion	67.4	81.6
Water	65.4	28.8
RMSD		
Bond length, Å	0.007	0.006
Bond angle, degrees	0.952	0.840

*Values in parentheses are for the highest-resolution shell.

with dimensions of $0.25 \times 0.15 \times 0.03$ mm^3 were obtained by successive microseeding (32). For the Puf3p:*COX17* site A (CUUGUAUAUA) complex, the well solution was 20% PEG4000, 0.1 M sodium citrate (pH 4.8), and 2% dextran sulfate. Diffraction-quality crystals with dimensions of $0.20 \times 0.12 \times 0.03$ mm^3 were obtained by a combined procedure of cross-seeding (original crystal seeds from a Puf3p:*COX17* site B complex crystal), microseeding, and macroseeding.

Crystals were flash-cooled in liquid nitrogen after incubation in cryoprotectant solution containing the well solution supplemented with 10% ethylene glycol. X-ray diffraction data for Puf3p:*COX17* site B and Puf3p:*COX17* site A were collected at the Advanced Photon Source Beamline ID-22 (wavelength 1.0 Å) and Rigaku RU-007HF (wavelength 1.5418 Å), respectively. The data were processed using HKL2000 (33). Data statistics are summarized in Table 2.

Structure Determination and Refinement. The structure of the Puf3p:*COX17* site B complex was determined by molecular replacement using the coordinates of the PUM1 structure (1M8Y) with the Phaser program (34). Swiss PDB Viewer (35) was used to thread the aligned Puf3p sequence onto the model, followed by manual model building using ''O'' (36). The model was refined using PHENIX (37) with noncrystallographic restraints for both protein and RNA. Parameters for the bases at positions 5 and 8, which use C2'-endo geometry, were modified based on C3'-endo restraints from CNS (38). The structure of the Puf3p:*COX17* site A complex was determined using the Puf3p:*COX17* site B complex structure model. Electron density maps revealed interpretable density for the RNA, with differences primarily in locations where the RNA bases differ. Both structures contain 3 Puf3p:RNA complexes in the asymmetric unit; we focus on the details of the Puf3p:*COX17* siteB complex (chains A and B), which was determined at higher resolution (2.5 Å). Most details are observed in all complexes with either RNA. The structures

were analyzed using MolProbity (39). Model and refinement statistics are summarized in Table 2. All φ–ψ torsion angles are within allowable regions of the Ramachandran plot, and 98% and 99% are in the favored regions for structures of Puf3p:*COX17* site B and Puf3p:*COX17* site A, respectively. There are no incorrect sugar puckers or RNA backbone conformations.

Electrophoretic Mobility Shift Assays. Equilibrium dissociation constants for Puf3p and S866A mutPuf3p proteins were determined by electrophoretic mobility shift binding assays. RNA oligonucleotides were obtained from Dharmacon and radiolabeled at the 5'-end using ^{32}P-γ-ATP (PerkinElmer Life Sciences) and T4 polynucleotide kinase (New England BioLabs) following the manufacturer's instructions. Puf4p was expressed and purified as described previously (26).

Binding reactions included radiolabeled target RNA and serially diluted concentrations of protein and were incubated overnight at 4 °C in buffer containing 10 mM Tris-HCl (pH 7.4), 100 mM NaCl, 2 mM MgCl$_2$, 3% glycerol, 5 μg/mL of heparin, 0.01% IGEPAL, and 6 mM β-mercaptoethanol. For the Puf3p-binding assays, we used 30 pM for the *COX17* site A, *COX17* site B, and A5U site B RNAs and 300 pM for the other RNA oligonucleotides. For the Puf4p binding assays, we used 100 pM Puf4p consensus and Puf4p consensus U(−2)C RNAs and 300 pM for the other RNA oligonucleotides. Reactions were loaded within 6 min after addition of Ficoll to 2.5% (vol/vol) and run on 20% 19:1 acrylamide:bisacrylamide gels with 0.5× TBE at 4 °C under 150 V constant voltage for 90 min. The gels were dried and then exposed to storage phosphor screens (GE Healthcare) and scanned on a Molecular Dynamics Typhoon phosphorimager (GE Healthcare). The intensities of bands corresponding to bound and free radiolabeled RNA were measured using GelEval (Frogsoft), and the data were plotted and analyzed using IgorPro (WaveMetrics). The equilibrium dissociation constants were calculated by fitting the plot of the fraction bound versus protein concentration to the Hill equation, assuming a Hill coefficient of 1. The mean and standard error of at least 3 independent experiments are reported. Statistical analyses were performed with GraphPad Prism software. A representative experiment is shown in Fig. S5. The conditions for the assay were established by testing the effect on K_d of varying incubation time (2–48 h), RNA concentration (10–300 pM), and time after the addition of loading buffer (5–15 min). No significant difference in K_d was detected under these conditions. Determination of the percentage of active protein was performed as described previously (40). Puf3p was 94% active, and Puf4p was 91% active; no corrections were made to the measured K_d.

In Vivo Analyses of mRNA Stability. *COX17* reporter constructs were generated on CEN plasmids and transformed into wild-type and puf3Δ yeast strains. mRNA half-life determinations were made by decay from steady-state experiments as described previously with minor modifications (41). In brief, yeast were grown to mid-log phase at 30 °C in galactose-containing media. Yeast were concentrated in media containing galactose and incubated for 30 min. Transcription of the reporters was terminated by the addition of glucose. Samples were collected and frozen. RNA was isolated using the MasterPure Yeast RNA Purification Kit (Epicentre Biotechnologies). Northern blot analysis was performed as described previously (42). Decay data were analyzed using GraphPad Prism software. Site-directed mutants of Puf3p that affect RNA binding and mRNA decay (29) are analyzed in Fig. S6.

1. Kimble J, Crittenden SL (2007) Controls of germline stem cells, entry into meiosis, and the sperm/oocyte decision in *Caenorhabditis elegans*. *Annu Rev Cell Dev Biol* 23:405–433.
2. Thompson B, Wickens M, Kimble J (2007) in *Translational Control in Biology and Medicine*, eds Mathews MB, Sonenberg N, Hershey JWB (Cold Spring Harbor Lab Press, Cold Spring Harbor, NY), pp 507–544.
3. Mendez R, Richter JD (2001) Translational control by CPEB: A means to the end. *Nat Rev Mol Cell Biol* 2:521–529.
4. Pique M, Lopez JM, Foissac S, Guigo R, Mendez R (2008) A combinatorial code for CPE-mediated translational control. *Cell* 132:434–448.
5. Licatalosi DD, et al. (2008) HITS-CLIP yields genome-wide insights into brain alternative RNA processing. *Nature* 456:464–469.
6. Jacobs Anderson JS, Parker R (2000) Computational identification of *cis*-acting elements affecting post-transcriptional control of gene expression in *Saccharomyces cerevisiae*. *Nucleic Acids Res* 28:1604–1617.
7. Olivas W, Parker R (2000) The Puf3 protein is a transcript-specific regulator of mRNA degradation in yeast. *EMBO J* 19:6602–6611.
8. Gerber AP, Herschlag D, Brown PO (2004) Extensive association of functionally and cytotopically related mRNAs with Puf family RNA-binding proteins in yeast. *PLoS Biol* 2:e79.
9. Garcia-Rodriguez LJ, Gay AC, Pon LA (2007) Puf3p, a Pumilio family RNA-binding protein, localizes to mitochondria and regulates mitochondrial biogenesis and motility in budding yeast. *J Cell Biol* 176:197–207.

10. Saint-Georges Y, et al. (2008) Yeast mitochondrial biogenesis: A role for the PUF RNA-binding protein Puf3p in mRNA localization. *PLoS ONE* 3:e2293.

11. Glerum DM, Shtanko A, Tzagoloff A (1996) Characterization of COX17, a yeast gene involved in copper metabolism and assembly of cytochrome oxidase. *J Biol Chem* 271:14504–14509.

12. Jackson JS, Jr., Houshmandi SS, Lopez Leban F, Olivas WM (2004) Recruitment of the Puf3 protein to its mRNA target for regulation of mRNA decay in yeast. *RNA* 10:1625–1636.

13. Wickens M, Bernstein DS, Kimble J, Parker R (2002) A PUF family portrait: 3′-UTR regulation as a way of life. *Trends Genet* 18:150–157.

14. Wharton RP, Aggarwal AK (2006) mRNA regulation by Puf domain proteins. *Sci STKE* 2006:pe37.

15. Bernstein D, Hook B, Hajarnavis A, Opperman L, Wickens M (2005) Binding specificity and mRNA targets of a *C. elegans* PUF protein, FBF-1. *RNA* 11:447–458.

16. Edwards TA, Pyle SE, Wharton RP, Aggarwal AK (2001) Structure of Pumilio reveals similarity between RNA and peptide-binding motifs. *Cell* 105:281–289.

17. Galgano A, et al. (2008) Comparative analysis of mRNA targets for human PUF-family proteins suggests extensive interaction with the miRNA regulatory system. *PLoS ONE* 3:e3164.

18. Macdonald PM (1992) The *Drosophila pumilio* gene: An unusually long transcription unit and an unusual protein. *Development* 114:221–232.

19. Opperman L, Hook B, DeFino M, Bernstein DS, Wickens M (2005) A single spacer nucleotide determines the specificities of two mRNA regulatory proteins. *Nat Struct Mol Biol* 12:945–951.

20. Stumpf CR, Kimble J, Wickens M (2008) A *Caenorhabditis elegans* PUF protein family with distinct RNA binding specificity. *RNA* 14:1550–1557.

21. Wang X, McLachlan J, Zamore PD, Hall TM (2002) Modular recognition of RNA by a human pumilio-homology domain. *Cell* 110:501–512.

22. Wang X, Zamore PD, Hall TM (2001) Crystal structure of a Pumilio homology domain. *Mol Cell* 7:855–865.

23. Zamore PD, Williamson JR, Lehmann R (1997) The Pumilio protein binds RNA through a conserved domain that defines a new class of RNA-binding proteins. *RNA* 3:1421–1433.

24. Zhang B, et al. (1997) A conserved RNA-binding protein that regulates sexual fates in the *C. elegans* hermaphrodite germ line. *Nature* 390:477–484.

25. Gupta YK, Nair DT, Wharton RP, Aggarwal AK (2008) Structures of human Pumilio with noncognate RNAs reveal molecular mechanisms for binding promiscuity. *Structure* 16:549–557.

26. Miller MT, Higgin JJ, Tanaka Hall TM (2008) Basis of altered RNA-binding specificity by PUF proteins revealed by crystal structures of yeast Puf4p. *Nat Struct Mol Biol* 15:397–402.

27. Lee MH, et al. (2007) Conserved regulation of MAP kinase expression by PUF RNA-binding proteins. *PLoS Genet* 3:e233.

28. Foat BC, Houshmandi SS, Olivas WM, Bussemaker HJ (2005) Profiling condition-specific, genome-wide regulation of mRNA stability in yeast. *Proc Natl Acad Sci USA* 102:17675–17680.

29. Houshmandi SS, Olivas WM (2005) Yeast Puf3 mutants reveal the complexity of Puf-RNA binding and identify a loop required for regulation of mRNA decay. *RNA* 11:1655–1666.

30. Ulbricht RJ, Olivas WM (2008) Puf1p acts in combination with other yeast Puf proteins to control mRNA stability. *RNA* 14:246–262.

31. DeLano WL (2002) *The PyMOL Molecular Graphics System* (DeLano Scientific, San Carlos, CA).

32. Zhu DY, Zhu YQ, Xiang Y, Wang DC (2005) Optimizing protein crystal growth through dynamic seeding. *Acta Crystallogr D* 61:772–775.

33. Otwinowski Z, Minor W (1997) Processing of X-ray diffraction data collected in oscillation mode. *Methods Enzymol* 276:307–326.

34. McCoy AJ, Grosse-Kunstleve RW, Storoni LC, Read RJ (2005) Likelihood-enhanced fast translation functions. *Acta Crystallogr D* 61:458–464.

35. Guex N, Peitsch MC (1997) SWISS-MODEL and the Swiss-PdbViewer: An environment for comparative protein modeling. *Electrophoresis* 18:2714–2723.

36. Jones TA, Zou J-Y, Cowan SW, Kjeldgaard M (1991) Improved methods for building protein models in electron-density maps and the location of errors in these models. *Acta Crystallogr A* 47:110–119.

37. Adams PD, et al. (2004) Recent developments in the PHENIX software for automated crystallographic structure determination. *J Synchrotron Radiat* 11:53–55.

38. Brünger AT, et al. (1998) Crystallography and NMR system: A new software suite for macromolecular structure determination. *Acta Crystallogr D* 54:905–921.

39. Davis IW, et al. (2007) MolProbity: All-atom contacts and structure validation for proteins and nucleic acids. *Nucleic Acids Res* 35:W375–W383.

40. Cheong C-G, Hall TMT (2006) Engineering RNA sequence specificity of Pumilio repeats. *Proc Natl Acad Sci USA* 103:13635–13639.

41. Coller JM, Tucker M, Sheth U, Valencia-Sanchez MA, Parker R (2001) The DEAD box helicase, Dhh1p, functions in mRNA decapping and interacts with both the decapping and deadenylase complexes. *RNA* 7:1717–1727.

42. Seay D, Hook B, Evans K, Wickens M (2006) A three-hybrid screen identifies mRNAs controlled by a regulatory protein. *RNA* 12:1594–1600.

43. Wang Y, Opperman L, Wickens M, Hall TMT (2009) Structural basis for specific recognition of multiple mRNA targets by a PUF regulatory protein. *Proc Natl Acad Sci USA*, 10.1073/pnas.0812076106.

BIOCHEMISTRY